IET Nanobiotechnology

Research Article

IET Journals
The Institution of Engineering and Technology

Biosynthesis of reusable and recyclable CuO@Magnetite@Hen Bone NCs and its antioxidant and antibacterial activities: a highly stable magnetically nanocatalyst for excellent reduction of organic dyes and adsorption of polycyclic aromatic hydrocarbons

ISSN 1751-8741
Received on 15th March 2018
Revised 17th August 2018
Accepted on 31st August 2018
E-First on 29th October 2018
doi: 10.1049/iet-nbt.2018.5014
www.ietdl.org

S. Mohammad Sajadi[1,2] ✉, Kamal Kolo[1], Samir M. Hamad[1,3], Sarbast A. Mahmud[4,5], Mohammad Pirouei[2], Keyvan Amjadian[2], Karzan M. Khalid[4]

[1]*Scientific Research Center, Soran University, P.O. Box 624, Soran, Kurdistan Regional Government, Iraq*
[2]*Department of Petroleumgeosciences, Faculty of Science, Soran University, PO Box 624, Soran, KRG, Iraq*
[3]*Research Center, Cihan University-Erbil, Iraq*
[4]*Department of Biology, Faculty of Science, Soran University, PO Box 624, Soran, KRG, Iraq*
[5]*Department of Pharmacy, Rwandz private technical institute, Rawanduz, Soran, KRG, Iraq*
✉ *E-mail: smohammad.sajadi@gmail.com*

Abstract: For the first time, through a fast, eco-friendly and economic method, the aqueous extract of the leaf of *Euphorbia corollate* was used to the green synthesis of the highly stable *CuO@Magnetite@Hen Bone* nanocomposites (NCs) as a potent antioxidant and antibacterial agent against *Pseudomonas aureus*, *Staphylococcus aureus*, *Escherichia coli* and *Klebsiella pneumoniae* pathogenic bacteria. The biosynthesised NCs were identified using the scanning electron microscopy (SEM), energy dispersive X-ray spectroscopy, elemental mapping, X-ray diffraction (XRD), Fourier transforms infrared spectroscopy and UV–vis analytical techniques. Also, the radical scavenging activity using (2,2-diphenyl-1-picrylhydrazyl) method was used to evaluate the antioxidant activity of the NCs. The stability of nanocatalyst was monitored using the XRD and SEM analyses after 30 days from its synthesis. Furthermore, its excellent catalytic activity, recycling stability, and high substrate applicability were demonstrated to the adsorption of the polycyclic aromatic hydrocarbons of the light crude oil from Shiwashok oil fields and destruction of methylene blue and methyl orange as harmful organic dyes at ambient temperature using UV–vis spectroscopy. Moreover, the green CuO@Magnetite@Hen Bone NCs were recovered and reused several times without considerable loss of its catalytic activity.

1 Introduction

Nanotechnology covers the creation and application of physicochemical and biological systems with unique features between single atoms or molecules to submicron dimensions, and also assimilation of the obtained nanostructures into larger systems, [1–3]. The metal and metal oxide nanoparticles (NPs) play an important role in medical sciences for their extensive surface which provides a large number of active sites per unit area compared to the parent metal. Up to now, several methods were discovered for the synthesis of metal NPs using toxic and harsh methods in which the accumulation of dangerous materials on nanosurface restricted their applications in some aspects such as medicine and pharmacology [4–7]. In recent years, many efforts developed to replace the previous methods of NPs synthesis with more eco-friendly ways using natural supporting materials that increase the stability of produced nanostructures by altering their sensitivity to oxygen, water, and other chemical entities [8]. Moreover, beside the cost effectiveness of natural supports, employment of them to produce of metal NPs is a suitable method to decrease the agglomeration of nanostructures [9–11].

Hen bone as an anti-agglomeration support is among the rare, simple accessible and efficient bio-templates which its matrix is mostly made up of a composite material incorporating the inorganic mineral from salts of calcium and phosphate in the chemical arrangement termed calcium hydroxyapatite ($Ca_{10}(PO_4)_6(OH)_2$) and collagen [12].

Todays, researchers interested in the screening and identification of new antioxidants from the plant sources. Antioxidant activity in plant extract is due to the redox potential of phytochemicals to quench the singlet and triplet oxygen, decomposing the peroxides or neutralising the free radicals. Higher bioactivities of NPs probably are due to the large surface of NPs and preferential adsorption of the bioactive materials such as bioactive phytochemicals from the plant onto their surface which strongly affected by the surface area, particle size and surface reactivity of the NPs [13–19].

The increasing applications of dyes and pigments in different aspects of human life are visible. For toxicity and carcinogenic characteristics of organic dyes, discovering and developing the efficient, simple and cost-effective treatment methods for the removal of them is a drastic requirement. Up to now, many studies allocated to the research on the elimination of organic dyes pollutants but these methods show some drawbacks and harsh conditions [20, 21].

A lot of number of reported literature confirmed the excellent ability of nanostructures in catalytic degradation of organic dyes for their large surface area. In fact, the dye degradation methods, including the green synthesised nanocatalysts do not present the side effects and difficulties containing the previous methods. A part of this research is to study the ability and efficiency of green synthesised CuO@Magnetite@Hen Bone nanocomposites (NCs)

in the destruction of methylene blue (MB) and methyl orange (MO) as harmful organic dyes [22–24].

Aromatic compounds are among the main pollutants with considerable hazards to living systems. Polycyclic aromatic hydrocarbons (PAHs) are lipophilic highly soluble compounds in organic solvents including fused aromatic rings with various toxicities produced mainly via incomplete combustion and pyrolysis of materials containing carbon and hydrogen, such as coal, oil, wood and petroleum products [25, 26]. Many reports confirmed that aromatic compounds especially PAHs are environmentally persistent poisons with carcinogenic, immune suppressant and mutagenic effects. The main sources of poly aromatic compounds are pyrogenic, petrogenic, and biological processes in which those produced from the petrogenic source are most widespread pollutants for considerable transportation, storage and application of crude oil and its products [27, 28]. Crude oil and its derived products are a complex mixture of hydrocarbons containing a large number of aromatic compounds especially PAHs. The precursors for PAHs found in crude oil are natural products, such as steroids, that have been chemically converted to aromatic hydrocarbons with passing the time [29–31]. During this research, we decided to study the catalytic ability of the green synthesised CuO@Magnetite@Hen Bone NCs to adsorb of aromatic hydrocarbons including PAHs from the Shiwashok crude oil. Shiwashok is among of the important oil fields of Kurdistan located in the city of Erbil, Iraqi Kurdistan, where it is under the authority of the Kurdish regional government.

Euphorbia plants are among the widely distributed plants ranging from herbs and shrubs to trees in tropical and temperate regions of all over the world. The plants of this family are known as antioxidant, antitumour, cytotoxic and antiviral natural source. The medicinal effect of *Euphorbiaceae* (spurge) family is for its rich phytochemical content including glycosides, alkaloids, polyphenols, flavonoids, coumarins, tannins, steroids and triterpenoids [32, 33].

Therefore, for the rich phytochemical content of this family, the extract of the *Euphorbia corollate* was used for the biosynthesis of NPs through a simple, fast and green method, as shown in Fig. 1.

However, to the best of our knowledge, we decided to in situ phytosynthesis of CuO@Magnetite@Hen Bone NCs using the *Euphorbia corollate* leaf extract to the study of its stability, antioxidant and antibacterial activities against common pathogenic bacteria. Further, the catalytic ability and recyclability properties of nanocomposite were monitored during the adsorption process of the aromatic contents of Shiwatshok crude oil and the destruction of MB and MO as harmful organic dyes at ambient temperature using UV–vis spectroscopy.

2 Experimental

2.1 Instruments and reagents

High-purity chemicals were purchased from the Merck and Aldrich chemical companies. X-ray diffraction (XRD) measurements were carried out using a Philips powder diffractometer type PW 1373 goniometer with a scanning rate of 2°/min in the 2θ range from 0° to 90°. UV–vis spectral analysis was recorded on a double-beam spectrophotometer (Super Aquarius) to monitor the surface plasmon resonance (SPR) signals of NPs. Morphology, particle dispersion and chemical composition of the prepared nanostructures were investigated by fast emission scanning electron microscopy (FE-SEM) (Cam scan MV2300) equipped with EDS (energy dispersive X-ray spectroscopy). Fourier transforms infrared (FT-IR) spectra were recorded on a Nicolet 370 FT/IR spectrometer (Thermo Nicolet, USA) using pressed KBr pellets. The antibacterial activity of green synthesis CuO@Magnetite@ Hen Bone NCs was studied using the disc diffusion method through Muller-Hinton media and by using the Chloramphenicol as a positive control. The *Pseudomonas aureus* (*P. aureus*), *Staphylococcus aureus* (*S. aureus*), *Escherichia coli* (*E. coli*) and *Klebsiella pneumoniae* (*K. pneumoniae*) were obtained from the Department of Biology, Soran University in KRG, Iraq.

Fig. 1 *Images of the Euphorbia corollate plant [34]*

2.2 Plant materials

The *Euphorbia corollate* plant was collected in summer 2017 in the Sarshive region in Iranian Kurdistan and identified by the Department of Agriculture from Kurdistan University, Sanandaj, Iran.

2.3 Preparation of the Euphorbia corollate leaf extract

50 g of dried leaf powder of the plant was boiled in 500 ml double distilled water for 30 min at 80°C then the aqueous extract was filtered and kept in the refrigerator for further steps of the study.

2.4 Biosynthesis of CuO NPs using the leaf extract of Euphorbia corollate

In a typical synthesis of CuO NPs, 50 ml of the aqueous extract of the plant was added dropwise to 50 ml of well-mixed 0.005 M aqueous solution of $CuCl_2$ with constant stirring at pH 9 and 70°C. After 5 min, the colour of the solution was changed due to excitation of SPR which indicates the formation of CuO NPs. Furthermore, the formation and stability of CuO NPs were monitored by UV–vis spectroscopy. The obtained solution of NPs centrifuged at 7000 rpm for 30 min to absolute separation at room temperature.

2.5 Green synthesis of magnetite using the leaf extract of Euphorbia corollate

50 ml of the aqueous mixture of $FeCl_3$ (0.008 M) and $FeCl_2$ (0.004 M) was added into the plant extract (50 ml) under reflux condition at pH 10 and 70°C. After 10 min, the green synthesised Fe_3O_4 NPs were separated using a permanent magnet and washed for several times then the dried sample was identified with SEM and XRD techniques. All the experiments were conducted at ambient temperature.

2.6 Green synthesis of CuO@Magnetite@Hen Bone NC

In a 250 ml conical flask, after pretreatment of hen bone, 1.2 g dried powdered bone was mixed with 100 ml plant extract then 0.6 g dried powder of the green synthesised magnetite (as obtained in Section 2.5) was added to the mixture while stirring at 80°C for 5 h. In the next step, 0.3 g biosynthesised dried powder of CuO NPs (as obtained in Section 2.4) was added to the mixture at the same condition for next 5 h. After absolutely mixing the components of the mixture, the obtained precipitate was dried and kept to further investigations.

2.7 Antimicrobial activity

The *P. aureus*, *S. aureus, E. coli* and *K. pneumoniae* bacterial strains were used during this study. Disc diffusion method was carried out by using a standard protocol [35]. The overnight bacterial cultures (100 µl) introduced over Muller-Hinton agar plates with a sterile glass rod and minimum inhibition concentration determined for each sample, as given in Table 1. Also, the positive and negative controls were Chloramphenicol and prepared discs using sterile distilled water. Briefly, 100 µl of the biosynthesised CuO NPs, magnetite NPs, CuO@Magnetite@Bone NCs and Chloramphenicol (at the same conditions) were loaded on provided discs (6 mm D) and dried before being placed on the agar. Each sample was tested in triplicate and the plates were inoculated

at 37°C for 24 h after incubation. Finally, the diameter of the inhibition zones was measured and tabulated.

2.8 Antioxidant activity using DPPH radical scavenging method

Antioxidant potential of the green fabricated NCs against 2,2-diphenyl-1-picrylhydrazyl (DPPH) was determined using the method described by Clarke *et al.* [36]. DPPH solution was prepared freshly, a 1: 1 ratio of the test sample and ascorbic acid (for comparison) at different concentrations were mixed with DPPH solution in a test tube and kept in the dark for 30 min, respectively. Absorbance at 517 nm was measured with a UV–vis spectrophotometer and compared to an ascorbic acid inhibition curve.

Further, the gallic acid was used as a control during the process for both samples. Each assay was carried out in triplicate. The percentage inhibition of the DPPH radical was calculated using the following equation:

$$\text{Radical scavenging activity (RSA\%) or inhibition (In\%)} = [(\text{Ac} - \text{At})/\text{Ac}] \times 100$$

where In is the DPPH inhibition (%), Ac is absorbance of control and At is absorbance of samples. The amounts of both required NCs and ascorbic acid to decrease the absorbance of DPPH by 50% (IC50) were calculated graphically as mean values ± standard deviations and compared together.

2.9 Catalytic activity of green synthesised CuO@Magnetite@Bone NCs for the reduction of MO

5 mg of CuO@Magnetite@Bone NCs was added to 25 ml of MO aqueous solution (3.1×10^{-5}) and the same volume of freshly prepared aqueous $NaBH_4$ (5.3×10^{-3}) while stirring at room temperature. The progress of the conversion reaction was then monitored by recording the time-dependent UV–vis absorption spectra of the mixture. At the end of the reaction, the catalyst was simply separated from the reaction system by brief centrifugation and washed successively with ethanol and dried for the next cycle.

2.10 Catalytic activity of green synthesised CuO@Magnetite@Bone NCs for the reduction of MB

7 mg of CuO@Magnetite@Bone NCs was added to 25 ml of both MB solutions (3.1×10^{-5}) and freshly prepared aqueous NaBH4 (5.3×10^{-3}) while stirring at room temperature. The progress of the reaction was monitored by recording the time-dependent UV–vis absorption spectra of the mixture. At the end of the reaction, the catalyst was simply separated from the reaction system by brief centrifugation and washed successively with ethanol and dried for the next cycle.

2.11 Adsorbent ability of green CuO@Magnetite@Bone NCs to the removal of the aromatic containing compounds of LCO

50 ml of the crude oil sample was mixed to 100 ml distilled water under reflux condition at 80°C for 30 min to remove the possible salts and inorganic interferences. After separation of the water phase, the oil sample was extracted using methanol: diethyl ether: benzene (3:1:1) to extract the aromatics. The different amounts of NCs were added to 20 ml of the extracted aromatics at reflux condition in 70°C for investigating the effect of the catalyst amount on the rate of the adsorption process, as given in Table 2. Finally, the nanocatalyst was separated from the mixture and washed with n-hexan and absolute ethanol then dried to be used in the next cycle. Also, the rest of the mixture monitored using the UV–vis spectroscopy to study the efficiency of the catalyst to adsorb the aromatic compounds.

3 Results and discussions

In this research, the *Euphorbia corollate* leaf extract was used as reducing media to the biosynthesis of both CuO and magnetite NPs and their immobilisation on hen bone as a natural support for the preparation of highly stable CuO@Magnetite@Bone NCs. Beside the stability of NCs, the antimicrobial activity and antioxidant properties of NCs using DPPH radical scavenging method were studied. The green synthesised CuO@Magnetite@Bone NCs were also used as an adsorbent to the removal of aromatic containing compounds of a crude oil sample from Shiwashok oil fields. The synthesised catalyst has been comprehensively characterised by various techniques such as FE-SEM, EDS, XRD, FT-IR and UV–vis spectroscopy.

3.1 Characterisation of Euphorbia corollate extract

Fig. 2 depicts the UV–vis spectrum of plant leaf extract. Fingerprint signals obtained by UV–vis spectroscopy at 360 nm (bond I) and 270 nm (bond II) are indicating the cinnamoyl and benzoyl systems of antioxidant phenolics inside the plant extract, respectively [35].

Moreover, the FT-IR signals around 3422, 1678, 1420 and 1200–1000 cm^{-1} are assigned to the OH, carbonyl group (C = O), stretching C = C aromatic ring and C–O vibrations, respectively, as shown in Fig. 3. Therefore, the FT-IR signals show a good correspondence to the UV–vis result to confirm the presence of phenolics inside the plant extract as bioreducing and capping agents.

3.2 Green synthesis and characterisation of CuO NPs using the Euphorbia corollate extract

As demonstrated using UV–vis and FT-IR techniques and also literature survey about the plant extract, the presence of reducing phytochemicals inside the *Euphorbia corollate* extract caused to the biosynthesis of CuO NPs according to the mechanism (see Fig. 4).

Fig. 5 shows the UV–vis monitoring of the formation and stability of green synthesised CuO NPs ranging from 5 min to 20 days (c). The maximum absorbance appeared around 550 nm due to the SPR indicates the reduction process and formation of NPs. As the spectrum depicted, the maximum absorbance of green synthesised NPs has no demonstrative changes in the position and symmetry of the absorption peak which indicates the relative stability of the product.

Fig. 6 shows the FE-SEM micrograph of biosynthesised CuO NPs. The micrograph depicted an approximately homogeneous spherical shape of NPs with an average size between 25 and 35 nm. Also, some agglomerations are shown in the micrograph. Therefore, the nanostructure of green synthesised NPs is confirmed using SEM micrograph.

Further, the elemental content of green synthesised CuO NPs including copper and oxygen approved through EDS analysis Fig. 7. The presence of O and Cu depicted by the EDS analysis absolutely confirm the formation of pure CuO NPs.

3.3 Identification of green synthesised Fe_3O_4 NPs using the Euphorbia corollate extract

The magnetite NPs synthesised by the extract of *Euphorbia corollate* and characterised using EDS and XRD analyses. As the XRD pattern of Fe_3O_4 NPs shows, the result has an excellent agreement with previously reported literature in which all peaks are associated with magnetite and there are no other peaks observed in its pattern indicating the presence of any impurity, as shown in Fig. 8. Moreover, based on the XRD patterns of CuO NPs and Fe_3O_4 NPs with respect to the *Sherrer's* equation the average crystallite size of the CuO NPs and Fe_3O_4 is found to be 16 and 75 nm, respectively.

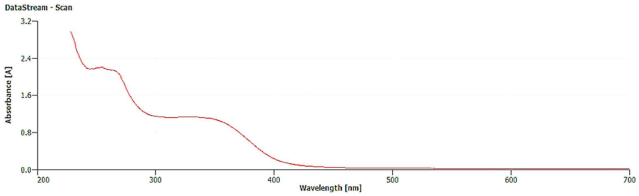

Fig. 2 *UV–vis spectroscopy of plant leaf extract*

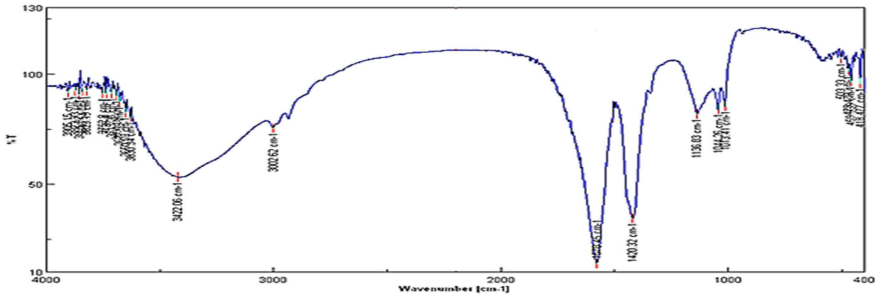

Fig. 3 *FT-IR signals of the plant leaf extract*

Table 1 Antibacterial activity of green CuO NPs, manetite NPs and CuO@Magnetite@Hen Bone NCs

Compounds	*P. aureus*, mm	*S. aureus*, mm	*E. coli*, mm	*K. pneumoniae*, mm
CuO NPs (1%)	28	35	32	28
Magnetite NPs (1%)	35	36	30	40
CuO@Magnetite@Hen Bone NCs (1%)	22	45	36	43
[a]Chloramphenicol	39	36	34	32

[a]C^+; Chloramphenicol disc diameter (positive control).

Table 2 Comparison of the catalytic ability of *NCs*

Dye	Entry	Catalyst	Time	Ref.
MO	1	Cu@SBA-15 NCs	5 min	[37]
	2	Ag NPs/seashell NCs	11 min	[38]
	3	Ag/TiO_2 NCs	9 min	[20]
	4	Ag NPs/clinoptilolite NCs	138 s	[39]
	5	Cu/eggshell NCs	2 min	[12]
	6	Pd/perlite NCs	10 min	[23]
	7	Ag NPs	24 h	[40]
	8	Au/PDMAEMA/RGO NCs	30 s	[41]
	9	GO/Pd NCs	5 min	[42]
	10	y 20%V–Bi_2(O, S)$_3$	150 s	[43]
	11	**CuO@Magnetite@Hen Bone**	**110 s**	**CS[a]**
MB	12	porous Cu microspheres	8 min	[36]
	13	SiNWAs-Cu	10 min	[44]
	14	Au/Fe_3O_4@C	10 min	[45]
	15	Ag NPs/seashell	2.5 min	[38]
	16	Ag/TiO_2 nanocomposite	70 s	[20]
	17	Ag NPs/clinoptilolite	40 s	[39]
	18	AgNPs on silica spheres	7.5 min	[12]
	19	Au_{core}–$PANI_{shell}$	5 min	[12]
	20	Cu nanocrystals	200 s	[12]
	21	Bentonite/Cu NPs	40 s	[22]
	22	Au nanorods	10 min	[46]
	23	rGO-SiW NCs	34 min	[47]
	24	Ag NPs@montmorillonite	9 min	[48]
	25	**CuO@Magnetite@Hen Bone NCs**	**20 s**	**CS[a]**

[a]CS: current study.

3.4 Green synthesis and characterisation of CuO@Fe_3O_4@Hen Bone NCs using the extract of Euphorbia corollate

In continuation of our previous studies in the application of plant extracts and natural supports in the preparation of nanostructures [44, 45, 49, 50], during this study, the CuO@Fe_3O_4@Hen Bone NCs were synthesised using the hen bone as a natural based support and *Euphorbia corollate* extract as antioxidant media.

The FT-IR analysis of NCs strongly confirmed the adsorption of phytochemicals on the surface of the nanostructure. The main peaks at 3390, 1704 and 1578 cm^{-1} are assigned to the functional groups of OH, C = O and C = C aromatic vibrations, respectively, as shown in Fig. 9. Therefore, the presence of bioactive phytochemicals on the nanosurface strongly justified the bioactivity of green synthesised NCs.

In the next step, the preparation of the CuO@Fe_3O_4@Hen Bone NCs was investigated by using XRD, SEM, EDS and Mapping methods. The surface morphology and size of the NCs were investigated using FE-SEM and TEM methods as depicted in Figs. 10 and 11, respectively. As concluded about the morphology of green NCs, the spherical morphology of NPs deposited on the surface of hen bone with the range size mostly between 10 and 85 nm.

Further, the EDS spectrum and elemental mapping images easily show the elemental structure and chemical composition of the NCs including well defined peaks of Ca, O, C, P, Fe and Cu, thereby confirming the successful anchoring of the CuO and magnetite NPs on the hen bone, as depicted in Figs. 12 and 13. Therefore, the SEM and EDS analyses proved the fabrication of the CuO@Fe_3O_4@Hen Bone NCs.

The crystallinity of green synthesised NCs was depicted by XRD, as shown in Fig. 11. As it is shown, the pattern revealed six characteristic peaks (in black colour) indexed the cubic structure of Fe_3O_4. The peaks correspond to the crystal planes of (110), (220), (311), (222), (400), (422) and (511) of crystalline Fe_3O_4. Further, the XRD spectrum of CuO NPs shown in blue colour in Fig. 14 including all the peaks associated with the crystalline planes of pure CuO NPs as (110), (111), (200), (202), (020), (202), (113), (311), (220) and (400). The XRD pattern of NCs also depicted the demonstrative peaks of ($Ca_{10}(PO_4)_6(OH)_2$) as the main component of NCs support (hen bone).

3.5 Evaluation of antimicrobial activity of green synthesised CuO@Magnetite@Hen Bone NCs

The antibacterial activity of the CuO NPs, magnetite NPs and finally green NCs was studied against *P. aureus*, *S. aureus*, *E. coli* and *K. pneumoniae* bacteria by disk diffusion method. The

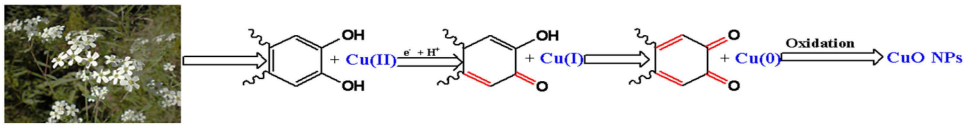

Fig. 4 *Mechanism of green synthesised CuO NPs*

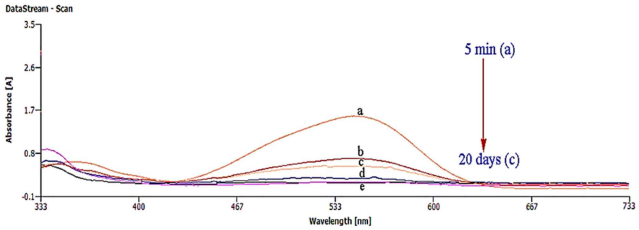

Fig. 5 *UV–vis spectra of green synthesised CuO NPs between 5 min (a) to 20 days (e)*

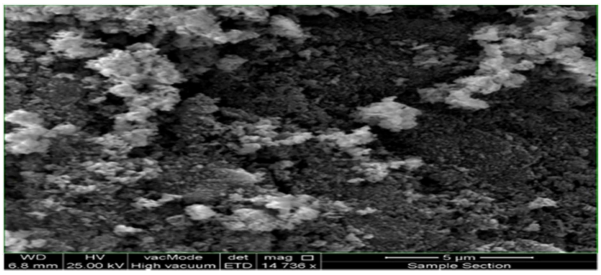

Fig. 6 *SEM micrograph of green synthesised CuO NPs*

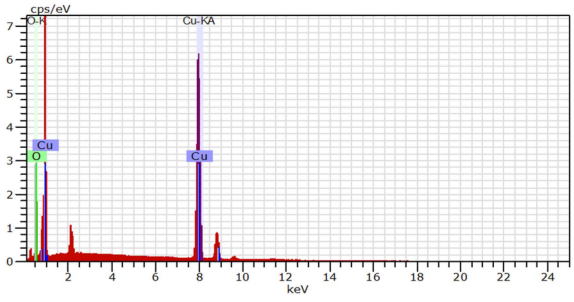

Fig. 7 *EDS spectrum of green synthesised CuO NPs*

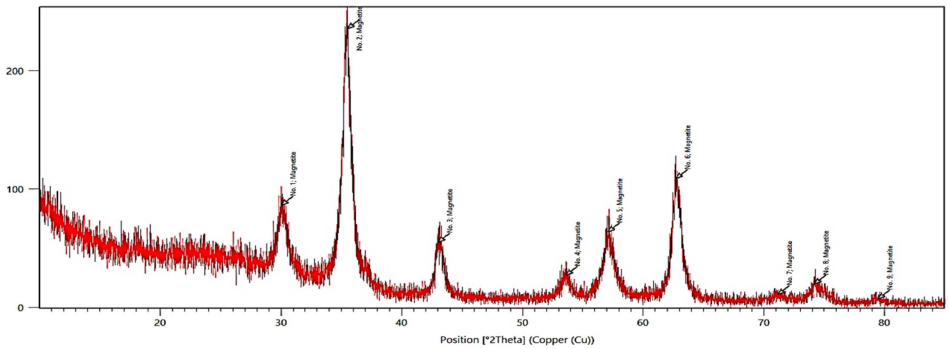

Fig. 8 *XRD pattern of green synthesised Fe_3O_4 NPs*

concentration of nanostructures used for this study was 1% (10 mg/ml) and results compared with Chloramphenicol as a positive control. All other test conditions were the same for each sample. The diameter of the appeared discs per millimetre as minimum protection zone was reported for each sample, as given in Table 1.

As it is shown in Table 1, the biosynthesised NCs showed more antibacterial activity against *S. aureus, E. coli* and *K. pneumoniae* bacteria than the NPs and control in the same conditions which probably refers to the more accumulation of the bioactive phytochemicals adsorbed on the extensive surface of NCs as confirmed through FT-IR spectra. Therefore, the study confirmed that the surface area of green synthesised nanostructures is an important factor in their antibacterial activity as larger surface area cased to adsorption of more bioactive phytochemicals and finally more antibacterial activity.

3.6 Antioxidant activity of biosynthesised CuO@Magnetite@Hen Bone NCs

This method is based on the reduction of DPPH, at 517 nm. In fact, antioxidants react with DPPH and pair off the odd electron of the radical to show a discolouring signal demonstrated the scavenging potential. This reaction is widely used to spectrophotometrically study of the RSA of the compounds. The parameter IC_{50} (efficient concentration value), is used for the interpretation of the DPPH method and defined as the concentration of substrate that causes

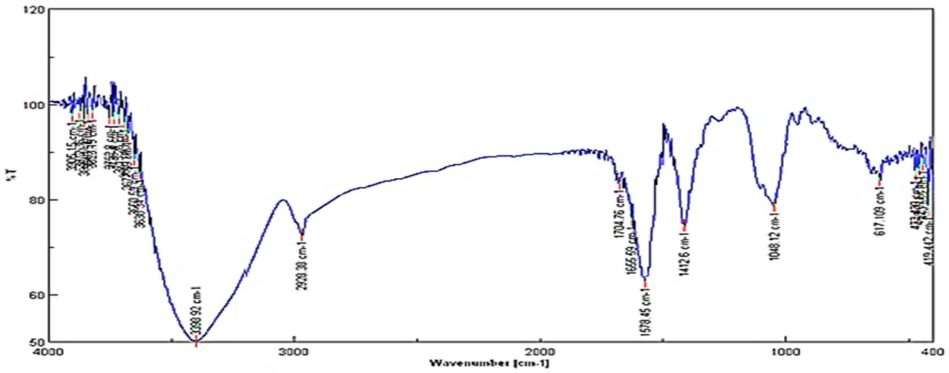

Fig. 9 *FT-IR spectrum of the green synthesised nanocomposite*

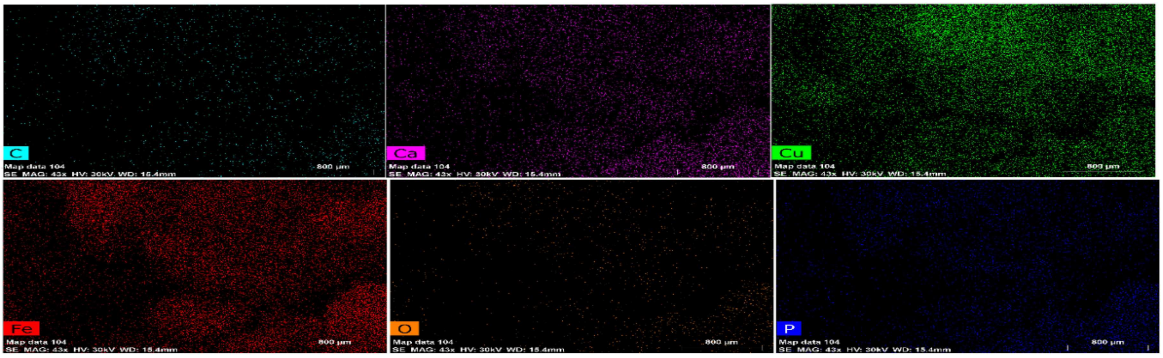

Fig. 10 *FE-SEM micrograph of green synthesised CuO@Fe$_3$O$_4$@Hen Bone NCs*

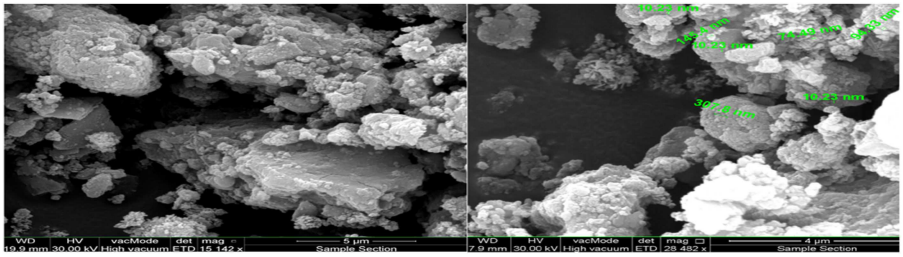

Fig. 11 *TEM images of the CuO@Magnetite@Hen Bone NCs*

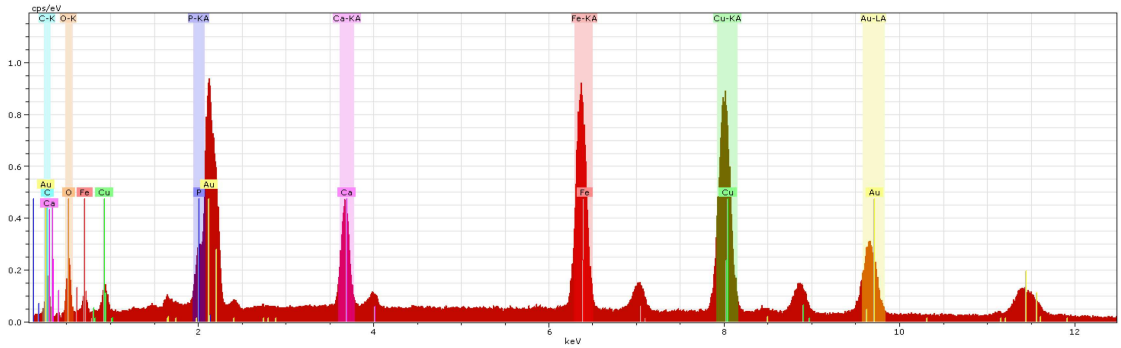

Fig. 12 *EDS spectrum of green synthesised CuO@Fe$_3$O$_4$@Hen Bone NCs*

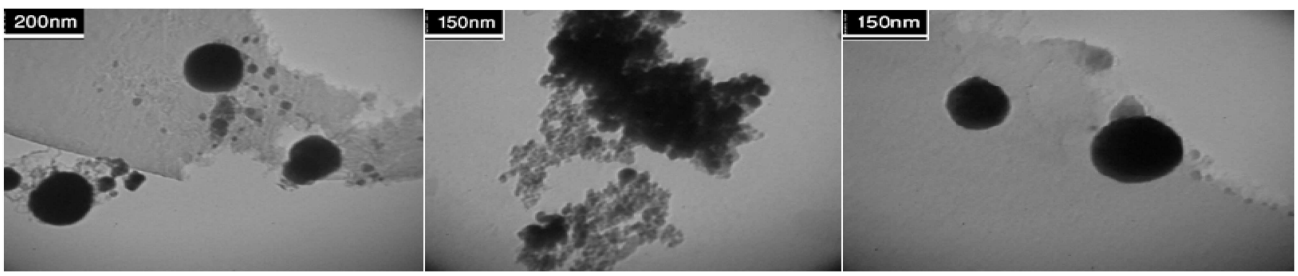

Fig. 13 *Elemental mapping of the green synthesised CuO@Magnetite@Hen Bone NC*

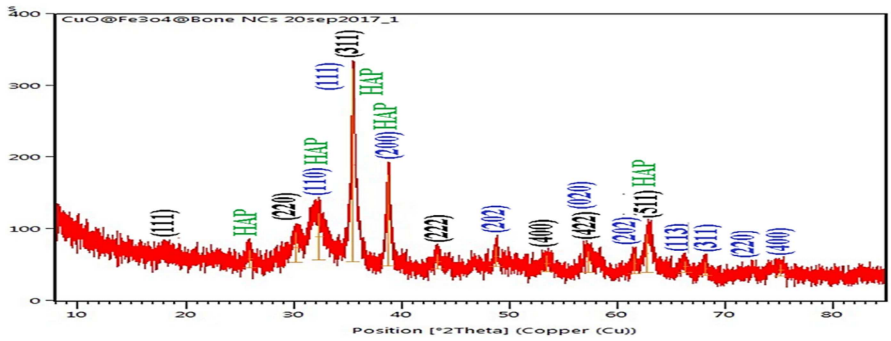

Fig. 14 *XRD pattern of green synthesised CuO@Magnetite@Hen Bone NC*

Table 3 Effect of different amounts of NCs on the reaction

Entry	Dye, M	$NaBH_4$, M	Catalyst, mg[a]	Time
1	MO	5.3×10^{-3}	3	3 min
2	MO	5.3×10^{-3}	5	110 s
3	MO	5.3×10^{-3}	8	150 s
4	MO	5.3×10^{-3}	10	195 s
5	MB	5.3×10^{-3}	1	3 min[b]
6	MB	5.3×10^{-3}	3	45 s
7	MB	5.3×10^{-3}	5	35 s
8	MB	5.3×10^{-3}	7	20 s

[a]CuO@Magnetite@Hen Bone NCs.
[b]Not completed.

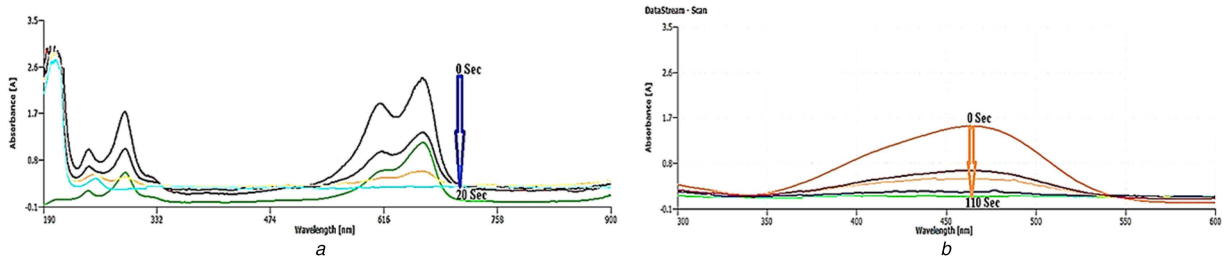

Fig. 15 *Evolution of the UV–vis spectra of dyes aqueous solution in the presence of green NCs*
(a) MB, ***(b)*** MO

50% loss of the DPPH activity. Following the study of antioxidant activity using this method for NCs and ascorbic acid against the gallic acid as control, the IC_{50} values calculated as 33.32 and 32.61 ppm for green synthesised NCs and ascorbic acid, respectively. Further the RSA% of the NCs in concentrations >350 ppm is clearly higher than the ascorbic acid in which this parameter is the highest at the maximum dose of 500 ppm (74%) at compared with ascorbic acid (64%) at the same concentration. The study of the antioxidant ability of the green NCs strongly demonstrated that a considerable amount of antioxidant phytochemicals deposited on the surface of the nanostructure, which causes an antioxidant property even more than a potent antioxidant compound such as ascorbic acid due to their ability to transfer of a hydrogen atom or an electron.

3.7 Reduction of MO and MB using CuO@Magnetite@Hen Bone NCs

During this research, we focused on the catalytic ability of the green NCs for the reduction of MO and MB in the presence of $NaBH_4$. The decolourisation process benefits from the adsorption of $NaBH_4$ onto the surface of catalyst and formation of metal hydride. In the next step, the organic dyes adsorb onto the surface of the catalyst and then reduced. Finally, the reduced dyes desorb from the catalyst surface to create a free space to continue of process to evaluate the performance of the NCs, the different amounts of catalyst were investigated, as shown in Table 3.

Table 3 shows that the best result for MO and MB reduction was obtained with 5 and 7 mg catalyst, respectively, in the presence of $NaBH_4$ and at room temperature. The complete degradation time of these organic dyes was 110 s for MO and 20 s for MB. The reduction process of MO and MB monitored spectrophotometrically by decreasing the maximum absorbance and removing the maxima while decolourising the organic dyes, as shown in Fig. 15.

The comparison of the ability and efficiency of NCs for the reduction of MO and MB dyes with some of the previous reports revealed that employing the green catalyst caused a shorter degradation time in contrast with the reported methods by other catalysts except for entry eight in Table 2.

During the degradation process, the reaction does not depend on the concentration of $NaBH_4$ but it roughly depends on the concentration of MB and MO dyes as a pseudo first-order kinetics mechanism. Also, in the absence of the catalyst, no degradation process is seen even after passing a lot of time while stirring and heating.

3.8 Catalytic ability of green synthesised CuO@Magnetite@Hen Bone NCs to adsorb the aromatic compounds of crude oil

The ability of NCs was tested to adsorb the aromatic compounds of crude oil including its PAHs. Initially, the process was optimised for the adsorption of aromatics of the crude oil in the presence of

Table 4 Effect of the catalyst amounts on the adsorption time of the crude oil aromatics

Entry	Catalyst	Crude oil aromatics, ml	Catalyst, mg	Time, min
1	CuO NPs	20	5	20
2	CuO NPs	20	7	20
3	CuO NPs	20	10	15
4	Fe_3O_4 NPs	20	7	20
5	Fe_3O_4 NPs	20	10	20
6	CuO@Magnetite@Hen Bone NCs	20	3	20[a]
7	CuO@Magnetite@Hen Bone NCs	20	5	10
8	CuO@Magnetite@Hen Bone NCs	20	7	10
9	CuO@Magnetite@Hen Bone NCs	20	10	5
10	hen bone (support)	20	10	45[b]
11	hen bone (support)	20	20	45[b]

[a]Few adsorbed
[b]Not adsorbed.

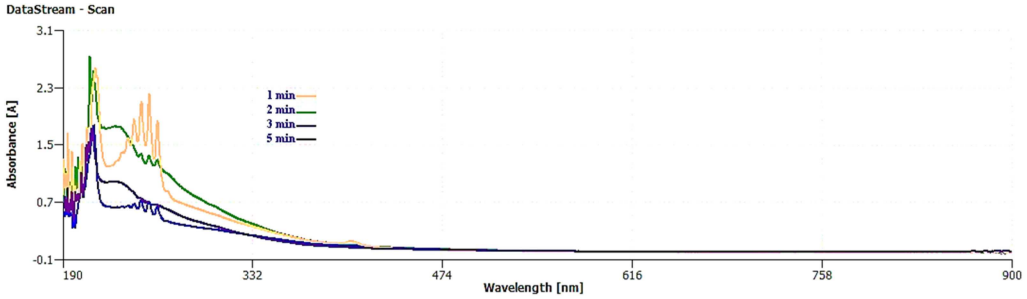

Fig. 16 *Adsorption of crude oil aromatics including PAHs using CuO@Magnetite@Hen Bone NCs (10 mg catalyst and 20 ml aromatic sample)*

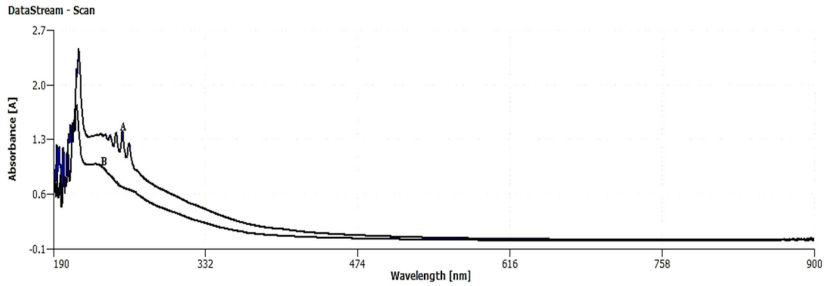

Fig. 17 *UV–vis spectroscopic detection of CuO@Magnetite@Hen Bone NCs reusability to adsorb the crude oil aromatic compounds; A: extracted aromatics, B: adsorption process after six times of recycling the catalyst*

different amounts of catalyst. According to Table 4, the best result is obtained using 10 mg of the catalyst. Also, it revealed that in the absence of a catalyst and only using the support as an adsorbent, no adsorption would occur even after 45 min (entries 10 and 11). Further, the other fractions of catalyst (CuO NPs and magnetite NPs) show less efficiency than the NC. According to the entry 6 in the mentioned table, the application of 3 mg of catalyst shows no considerable adsorption signal even after 20 min (entry 6) and finally as Table 2 shows, the time of the adsorption process decreases with increasing the amount of the catalyst.

Fig. 16 clearly depicts that the application of 10 mg CuO@Magnetite@Hen Bone NCs (Table 4, entry 9) shows a good potential to absorb the aromatic content of the crude oil at different times in which after 5 min there was no considerable amounts of aromatics can be detected using UV–vis technique.

According to the FT-IR spectrum of biosynthesised NCs (Fig. 6) and intensity of its signals, a good concentration of phytochemicals has been adsorbed on NCs surface. These phytochemicals beside the enhancement of the synergistic effect of the catalyst and its surface activity probably captured the aromatic compounds of the crude oil including PAHs through the formation of chemical bonds on the surface of nanocatalyst and removing them from the sample media.

3.9 Recyclability of the CuO@Magnetite@Hen Bone NCs

Beside the benefits of the green synthesised catalyst such as simple preparation, using the green source, bioactivity, cost effectiveness and stability, its simple separation from the reaction mixture and recycling with no significant loss of its catalytic activity is of great importance. The reusability of the catalyst was investigated for both organic dyes degradation and removal of aromatic compounds containing PAHs from the crude oil sample of Shiwashok oil field. As shown in Fig. 17, the adsorbent nanocatalyst could be reused for the aromatics removal process at least for six times without loss of its adsorption ability.

After completion of the reaction, the catalyst was easily separated and recovered conveniently by filtration from the reaction mixture and washed with n-hexan and finally dried to the next cycle of the process in which the recyclability of the catalyst was monitored using the XRD analysis. As shown in Fig. 18, the XRD analysis of the catalyst after six times of reusing to adsorb the aromatic compounds of the crude oil shows a very good crystallinity nature with no significant changes in morphology and the position and intensity of the main signals.

Furthermore, the reusability and recyclability of the catalyst for organic dyes degradation process was monitored using UV–vis spectroscopy and SEM micrograph after five times of its reusing. After each cycle of the reaction, the catalyst was easily separated and recovered conveniently by filtration from the reaction mixture,

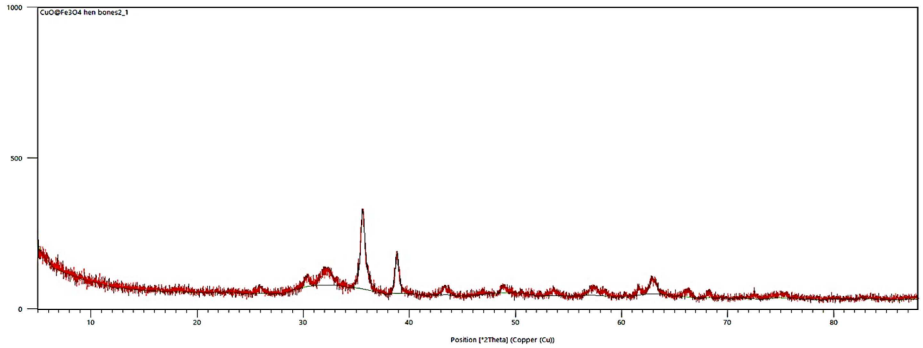

Fig. 18 *XRD pattern of recycled NCs after six times of aromatic removal process*

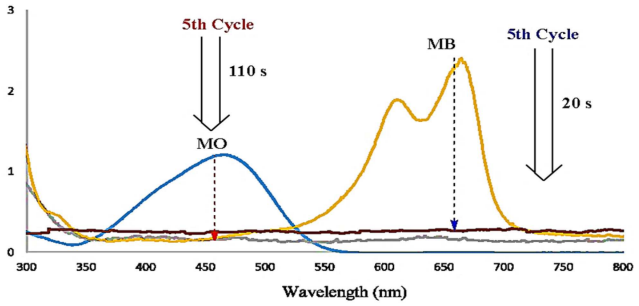

Fig. 19 *UV–vis spectroscopic monitoring of the CuO@Magnetite@Hen Bone NCs reusability after a fifth cycle of reaction for organic dyes destruction*

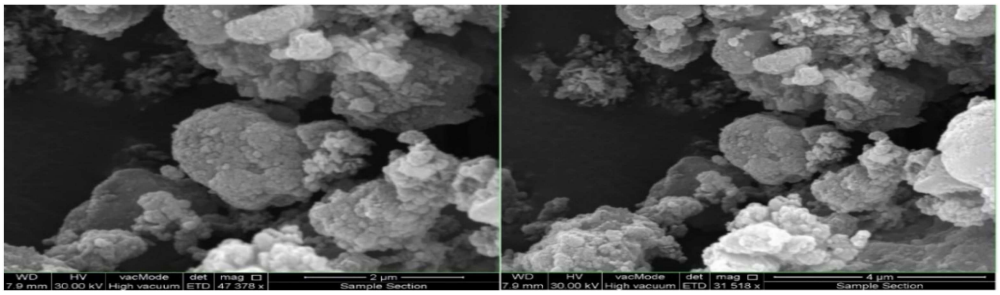

Fig. 20 *FE-SEM of the CuO@Magnetite@Hen Bone NCs recyclability after a fifth cycle of the reaction for organic dyes degradation*

washing with hot methanol and finally dried to use in the next cycle of the process. Fig. 19 shows the UV–vis monitoring of the catalyst in MO and MB dyes destruction. According to the figure, there is no changes in the shape, symmetry, maxima of the UV signals and adsorption ability of the catalyst in dyes degradation process even after a fifth cycle of the reaction, therefore, it shows excellent reusability in mentioned process.

Also, for more convenience, the catalyst morphological changes after its frequent recycling were monitored using the SEM technique. Fig. 20 demonstrates the high stability and turnover of the catalyst under operating conditions. The SEM analysis of recycled NCs shows that the particles are identical in morphology, shape and size even after the fifth run; therefore, it seems that green synthesised adsorbent is unchanged during the reaction process.

4 Conclusions

Through this study, we proposed a green, simple, efficient and economic strategy for the preparation of CuO@Magnetite@Hen Bone NCs using the bioreductant content of *Euphorbia corollate* extract. The green synthesised nanostructure was absolutely characterised using XRD, SEM, TEM, EDS, elemental mapping and FT-IR analytical techniques in which the FT-IR spectrum demonstrates the deposition of bioactive phytochemicals on the surface of the catalyst. The antimicrobial and antioxidant ability of the nanocatalyst was detected and results confirmed a very good bioactivity for the catalyst concerning the mentioned properties. The bioactive nanocatalyst used to adsorb the aromatic constituents, including PAHs from the crude oil of Shiwashok oil field under a mild condition in which demonstrates a high level of adsorption as monitored by UV–vis spectroscopy. Further, it was applied for the degradation process of MO and MB under a mild condition which the ability and efficiency of the catalyst were highly demonstrated. Finally, the reusability and recyclability of the catalyst for both processes were detected and its highly potential confirmed even after fifth or sixth cycle of the process without losing its catalytic activity.

5 Acknowledgments

The authors of this study highly appreciate Soran University for financial support of this project.

6. References

[1] González, C.R., Villalba, P.V., Salas, P., *et al.*: 'Green synthesis of nanosilver-decorated graphene oxide sheets', *IET Nanobiotech.*, 2016, **10**, p. 301

[2] Saran, M., Vyas, S., Mathur, M., *et al.*: 'Green synthesis and characterisation of CuNPs: insights into their potential bioactivity', *IET Nanobiotech.*, 2018, **12**, p. 357

[3] Busi, S., Rajkumari, J., Ranjan, B., *et al.*: 'Green rapid biogenic synthesis of bioactive silver nanoparticles (AgNPs) using *Pseudomonas aeruginosa*', *IET-Nanobiotech.*, 2014, **8**, p. 267

[4] Hosseinkhani, M., Montazer, M., Eskandarnejad, S., *et al.*: 'Simultaneous in situ synthesis of nano silver and wool fiber fineness enhancement using sulphur based reducing agents', *Colloids Surf. A*, 2012, **415**, p. 431

[5] Meftahizade, H.: 'Evaluation of antibacterial activity and wound healing of *Pistacia atlantica* and *Pistacia khinjuk*', *J. Med. Plants Res.*, 2011, **17**, p. 4310

[6] Schmid, G.: 'Large clusters and colloids. Metals in the embryonic state', *Chem. Rev.*, 1992, **92**, p. 1709

[7] Li, F., Zhang, B., Dong, S., *et al.*: 'A novel method of electrodepositing highly dispersed nano palladium particles on glassy carbon electrode', *Electrochem. Acta*, 1997, **42**, p. 2563

[8] Kim, W., Park, J., Jang, Y., *et al.*: 'Synthesis of monodisperse palladium nanoparticles', *Nano Lett.*, 2003, **3**, p. 1289

[9] Nemamcha, A., Rehspringer, J.: 'Synthesis of palladium nanoparticles by sonochemical reduction of palladium(II) nitrate in aqueous solution', *J. Phys. Chem. B*, 2006, **110**, p. 383

[10] Nasrollahzadeh, M., Sajadi, S.M., Maham, M., *et al.*: 'In situ green synthesis of Cu nanoparticles supported on natural natrolite zeolite for the reduction of 4-nitrophenol, Congo red and methylene blue', *IET Nanobiotech.*, 2017, **11**, p. 538

[11] Kiamehr, M., Alipour, B., Nasrollahzadeh, M., *et al.*: 'Catalytic reduction of 2,4-dinitrophenylhydrazine by cuttlebone supported Pd NPs prepared using *Conium maculatum* leaf extract', *IET Nanobiotech.*, 2018, **12**, p. 217

[12] Nasrollahzadeh, M., Sajadi, S.M., Hatamifard, A.: 'Waste chicken eggshell as a natural valuable resource and environmentally benign support for biosynthesis of catalytically active Cu/eggshell, Fe_3O_4/eggshell and Cu/Fe_3O_4/eggshell nanocomposites', *Appl. Catal. B*, 2016, **191**, p. 209

[13] Phull, A.R., Abbas, Q., Ali, A., *et al.*: 'Antioxidant, cytotoxic and antimicrobial activities of green synthesized silver nanoparticles from crude extract of *Bergenia ciliate*', *Future J Pharm Sci.*, 2016, **2**, p. 31

[14] Zhang, W., Wang, S.Y.: 'Antioxidant activity and phenolic compounds in selected herbs', *J. Agric. Food Chem.*, 2001, **49**, p. 5165

[15] Atarod, M., Nasrollahzadeh, M., Sajadi, S.M.: 'Green synthesis of a Cu/reduced graphene oxide/Fe_3O_4 nanocomposite using *Euphorbia wallichii* leaf extract and its application as a recyclable and heterogeneous catalyst for the reduction of 4-nitrophenol and rhodamine B', *RSC Adv.*, 2005, **5**, p. 91532

[16] Hollman, P.C.H., Arts, I.C.W.: 'Flavonols, flavones and flavanols – nature, occurrence and dietary burden', *J. Sci. Food Agric.*, 2000, **80**, p. 1081

[17] Lindley, M.G.: 'The impact of food processing on antioxidants in vegetable oils, fruits and vegetables', *Trends Food Sci. Technol.*, 1998, **9**, p. 336

[18] Colbert, L.B., Decker, E.A.: 'Antioxidant activity of an ultrafiltration permeate from acid whey', *J. Food Sci.*, 1991, **56**, p. 1248

[19] Antolovich, M., Prenzler, P.D., Patsalides, E., *et al.*: 'Methods for testing antioxidant activity', *Analyst*, 2002, **127**, p. 183

[20] Atarod, M., Nasrollahzadeh, M., Sajadi, S.M.: '*Euphorbia heterophylla* leaf extract mediated green synthesis of Ag/TiO_2 nanocomposite and investigation of its excellent catalytic activity for reduction of variety of dyes in water', *J. Colloid Interface Sci.*, 2016, **462**, p. 272

[21] Nasrollahzadeh, M., Sajadi, S.M., Khalaj, M.: 'Green synthesis of copper nanoparticles using aqueous extract of the leaves of *Euphorbia esula* L and their catalytic activity for ligand-free Ullmann-coupling reaction and reduction of 4-nitrophenol', *RSC Adv.*, 2014, **4**, p. 47313

[22] Issaabadi, Z., Nasrollahzadeh, M., Sajadi, S.M.: 'Green synthesis of the copper nanoparticles supported on bentonite and investigation of its catalytic activity', *J. Clean Prod.*, 2017, **142**, p. 3584

[23] Maryami, M., Nasrollahzadeh, M., Mehdipour, E., *et al.*: 'Green synthesis of the. Pd/perlite nanocomposite using *Euphorbia neriifolia* L. leaf extract and evaluation of its catalytic activity', *Sep. Sci. Technol.*, 2017, **184**, p. 298

[24] Crini, G.: 'Non-conventional low-cost adsorbents for dye removal: a review', *Bioresour. Technol.*, 2006, **97**, p. 1061

[25] Abdel-Shafy, H.I., Mansour, M.S.M.: 'A review on polycyclic aromatic hydrocarbons: source, environmental impact, effect on human health and remediation', *Egypt. J. Pet.*, 2016, **25**, p. 107

[26] He, J., Wen, Y., Ti, H.W., *et al.*: 'Investigation on modes of toxic action to rats based on aliphatic and aromatic compounds and comparison with fish toxicity based on exposure routes', *Chemosphere*, 2015, **128**, p. 111

[27] Dat, N.D., Chang, M.B.: 'Review on characteristics of PAHs in atmosphere, anthropogenic sources and control technologies', *Sci. Total Environ.*, 2017, **609**, p. 682

[28] Orisakwe, O.E., Lgweze, Z.N., Okolo, K.O., *et al.*: 'Human health hazards of poly aromatic hydrocarbons in Nigerian smokeless tobacco', *Toxicol Rep.*, 2015, **2**, p. 1019

[29] Babich, I.V., Moulijn, J.A.: 'Science and technology of novel processes for deep desulfurization of oil refinery streams', *Fuel*, 2003, **82**, p. 607

[30] Ma, X.L., Sakanishi, K., Isoda, T., *et al.*: 'Quantum chemical calculation on the desulfurization reactivities of heterocyclic sulfur compounds', *Energy Fuel*, 1995, **9**, p. 33

[31] Siddiqui, S.U., Ahmed, K.: 'Methods for desulfurization of crude oil: a review', *Sci. Int.*, 2016, **28**, p. 1169

[32] Sajadi, S.M., Salaryan, P., Enayati, A.: 'Optimal extraction method of phenolics from the root of *Euphorbia condylocarpa*', *Chem. Nat. Compd.*, 2011, **47**, p. 434

[33] Jasbi, A.R.: 'Chemistry and biological activity of secondary metabolites in *Euphorbia* from Iran', *Phytochemistry*, 2006, **67**, p. 1977

[34] http://www.nichegardens.com/catalog/item.php?id=134

[35] Madan, H.R., Sharma, S.C., Suresh, D., *et al.*: 'Facile green fabrication of nanostructure ZnO plates, bullets, flower, prismatic tip, closed pine cone: their antibacterial, antioxidant, photoluminescent and photocatalytic properties', *Acta Mol. Biomol. Spectrosc.*, 2016, **152**, p. 404

[36] Clarke, G., Ting, K.N., Wiart, C., *et al.*: 'High correlation of 2,2-diphenyl-1-picrylhydrazyl (DPPH) radical scavenging, ferric reducing activity potential and total phenolics content indicates redundancy in use of all three assays to screen for antioxidant activity of extracts of plants from the Malaysian rainforest', *Antioxidants*, 2013, **2**, p. 1

[37] Ghosh, B.K., Hazra, S., Nak, B., *et al.*: 'Preparation of Cu nanoparticle loaded SBA-15 and their excellent catalytic activity in reduction of variety of dyes', *Powder Technol.*, 2015, **269**, p. 371

[38] Rostami-Vartooni, A., Nasrollahzadeh, M., Alizadeh, M.: 'Green synthesis of seashell supported silver nanoparticles using *Bunium persicum* seeds extract: application of the particles for catalytic reduction of organic dyes', *J. Colloid Interf. Sci.*, 2016, **470**, p. 268

[39] Khodadadi, B., Bordbar, M., Faal, A.Y., *et al.*: 'Green synthesis of Ag nanoparticles/clinoptilolite using *Vaccinium macrocarpon* fruit extract and its excellent catalytic activity for reduction of organic dyes', *J. Alloys Compd.*, 2017, **719**, p. 82

[40] Joyti, K., Singh, A.: 'Green synthesis of nanostructured silver particles and their catalytic application in dye degradation', *J. Genet. Eng. Biotechnol.*, 2016, **14**, p. 311

[41] Mogha, N.K., Gosian, S., Masram, D.T.: 'Gold nanoworms immobilized graphene oxide polymer brush nanohybrid for catalytic degradation studies of organic dyes', *Appl. Surf. Sci.*, 2017, **396**, p. 1427

[42] Omidvar, A., Jaleh, B., Nasrollahzadeh, M.: 'Preparation of the GO/Pd nanocomposite and its application for the degradation of organic dyes in water', *J. Colloid Interf. Sci.*, 2017, **496**, p. 44

[43] Abay, A.K., Kuo, D.H., Chen, X., *et al.*: 'A new V-doped $Bi_2(O,S)_3$ oxysulfide catalyst for highly efficient catalytic reduction of 2-nitroaniline and organic dyes', *Chemosphere.*, 2017, **189**, p. 21

[44] Bhat, S.V., Nagasampagi, B.A., Sivakumar, M.: '*Chemistry of natural products*' (Narosa publishing house, New delhi, 2005), p. 585

[45] Nasrollahzadeh, M., Momeni, S.S., Sajadi, S.M.: 'Green synthesis of copper nanoparticles using *Plantago asiatica* leaf extract and their application for the cyanation of aldehydes using $K_4Fe(CN)_6$', *J. Colloid Interface Sci.*, 2017, **506**, p. 471

[46] Bhatt, C.S., Nagaraj, B., Suresh, A.K.: 'Nanoparticles-shape influenced high-efficient degradation of dyes: comparative evaluation of nano-cubes vs nano-rods vs nano-spheres', *J. Mol. Liq.*, 2017, **242**, p. 958

[47] Ucar, A., Findik, M., Gubbuk, H., *et al.*: 'Catalytic degradation of organic dye using reduced graphene oxide–polyoxometalate nanocomposite', *Mater. Chem. Phys.*, 2017, **196**, p. 21

[48] Wang, N., Hu, Y.X., Zhang, Z.: 'Sustainable catalytic properties of silver nanoparticles supported montmorillonite for highly efficient recyclable reduction of methylene blue', *Appl Clay Sci.*, 2017, **150**, p. 47

[49] Maham, M., Nasrollahzadeh, M., Sajadi, S.M., *et al.*: 'Biosynthesis of Ag/reduced graphene oxide/Fe_3O_4 using *Lotus garcinii* leaf extract and its application as a recyclable nanocatalyst for the reduction of 4-nitrophenol and organic dyes', *J. Colloid Interface Sci.*, 2017, **497**, p. 33

[50] Sajadi, S.M., Nasrollahzadeh, M.: 'Preparation of the Ag/RGO nanocomposite by use of *Abutilon hirtum* leaf extract: a recoverable catalyst for the reduction of organic dyes in aqueous medium at room temperature', *Int. J. Hydrog. Energy*, 2016, **41**, p. 21236